

AperTO - Archivio Istituzionale Open Access dell'Università di Torino

Downregulation of p53-inducible microRNAs 192, 194, and 215 impairs the p53/MDM2 autoregulatory loop in multiple myeloma development.

This is the author's manuscript

Original Citation:

Availability:

This version is available <http://hdl.handle.net/2318/88438> since

Terms of use:

Open Access

Anyone can freely access the full text of works made available as "Open Access". Works made available under a Creative Commons license can be used according to the terms and conditions of said license. Use of all other works requires consent of the right holder (author or publisher) if not exempted from copyright protection by the applicable law.

(Article begins on next page)



UNIVERSITÀ DEGLI STUDI DI TORINO

This is an author version of the contribution published on:

Questa è la versione dell'autore dell'opera:

[Cancer Cell. 2010 Oct 19;18(4):367-81. doi: 10.1016/j.ccr.2010.09.005.]

The definitive version is available at:

La versione definitiva è disponibile alla URL:

[<http://www.ncbi.nlm.nih.gov/pmc/articles/PMC3561766/pdf/nihms432681.pdf>]

Down-regulation of p53-inducible microRNAs 192, 194 and 215 impairs the p53/MDM2 auto-regulatory loop in multiple myeloma development

Flavia Pichiorri, Sung-Suk Suh, Alberto Rocci, Luciana De Luca, Cristian Taccioli, Ramasamy Santhanam, Zhou Wenchao, Don M. Benson, Jr, Craig Hofmainster, Hansjuerg Alder, Michela Garofalo, Gianpiero Di Leva, Stefano Volinia, Huey-Jen Lin, Danilo Perrotti, Michael Kuehl, Rami I. Aqeilan, Antonio Palumbo, Carlo M. Croce

Summary

In multiple myeloma (MM), an incurable B-cell neoplasm, mutation or deletion of p53 is rarely detected at diagnosis. Using small-molecule inhibitors of MDM2, we provide evidence that miR-192, 194 and 215, which are down-regulated in a subset of newly diagnosed MMs, can be transcriptionally activated by p53 and then modulate MDM2 expression. Furthermore, ectopic re-expression of these miRNAs in MM cells increases the therapeutic action of MDM2 inhibitors *in vitro* and *in vivo* by enhancing their p53-activating effects. In addition, miR-192 and 215 target the IGF pathway, preventing enhanced migration of plasma cells into bone marrow. The results suggest that these miRNAs are positive regulators of p53 and that their down-regulation plays a key role in MM development.

Significance

Therapeutic activation of p53 may be particularly appropriate for treatment of the ~50% of hematopoietic malignancies with intact *TP53*. We describe a signaling pathway in which miR-192, 194 and 215 are regulators of the MDM2/p53 auto regulatory loop, controlling the balance between p53 and MDM2 expression. Hypermethylation of the miR-194-2-192 cluster promoter in MM cell lines suggests that epigenetic down-regulation of these miRNAs, which leads to increased MDM2 mRNA and protein expression, decreases the ability of p53 to down-modulate MDM2 expression, thus tipping the regulatory loop in favor of MDM2. Exploring these miRNAs as enhancers in the pharmacological activation of the p53 pathway in MM cells might open avenues for miRNA-targeted therapies and MM treatment.

Introduction

The tumor suppressor p53 is frequently inactivated by mutations or deletions in cancer. p53 acts as a potent transcription factor and can be activated in response to diverse stresses, leading to induction of cell-cycle arrest, apoptosis or senescence (Junttila et al., 2009; Xue et al., 2007). Although regulation of the p53 pathway is not fully understood at the molecular level, it has been well established that activated p53 suppresses cancer progression, underlining why cancer cells have developed multiple mechanisms to disable p53 function (Danovi et al., 2004; Ventura et al., 2007). In human tumors that retain wild-type (WT) p53 (Junttila et al., 2009; Lane, 2001) p53 can be antagonized by murine double minute 2 (MDM2), a negative regulator of p53 that is also overexpressed in many human tumors, offering a therapeutic strategy (Dickens et al., 2009; Brown et al., 2009). It has been reported that inhibiting MDM2 expression can re-activate p53 in cancer cells, leading to their demise (Dickens et al., 2009; Saha et al., 2010).

TP53 mutation is rarely detected at diagnosis in many hematological cancers such as multiple myeloma (MM), acute myeloid leukemia, chronic lymphocytic leukemia and Hodgkin's disease (HD). Thus, numerous reports have shown that therapeutic induction of p53 might be particularly suitable for the treatment of hematological malignancies (Saha et al., 2010). Among them, multiple myeloma (MM) is a currently incurable plasma cell proliferative disorder that results in considerable morbidity and mortality (Kuehl et

al., 2002; Fonseca et al., 2009). MM develops from a benign condition called monoclonal gammopathy of undetermined significance (MGUS) (Weiss et al., 2009). Individuals with MGUS often remain stable for years and do not require treatment. However, for unknown reasons, this benign condition can evolve into MM at a rate of ~1% per year, with some MMs developing after many years (Kuehl et al., 2002; Fonseca et al., 2009).

In MGUS and in the majority of newly diagnosed MM cases *TP53* is WT (Kuehl et al., 2002; Chng et al., 2007) and the protein is rarely detectable (Stuhmer et al. 2006). Interestingly, in MM cells, expression of p53 protein levels can be rescued by antagonizing MDM2. Several reports have focused on the p53-mediated apoptotic pathway, upon endogenous p53 protein re-expression by the small-molecule MDM2 antagonists (Nutlins) and target genes which may be involved in p53-dependent apoptosis in MM cells have been identified (Stuhmer et al. 2006).

MicroRNAs are an abundant class of short, non protein-coding RNAs that mediate the regulation of target genes posttranscriptionally and that have emerged as master regulators in diverse physiologic and pathologic processes (Bartel, 2004), and oncogenesis (Croce, 2008). Recently, microRNAs (miRNAs) have been reported to be directly transactivated by p53 (He et al, 2007). miRNAs have also been shown to target p53 and/or components of p53 regulatory pathways, thereby directly and/or indirectly affecting its activities (Park et al., 2009; Zhang et al., 2009). We previously published the global miRNA-expression profiles of MM and MGUS, and contrasted these profiles with those of normal plasma cells (PCs) (Pichiorri et al., 2008). The findings defined a miRNA signature related to expression and regulation of proteins associated with malignant transformation of PCs, such as p53 (Pichiorri et al., 2008). We have now examined the regulation and functional roles of miRNAs in MM development using small-molecule inhibitors of MDM2.

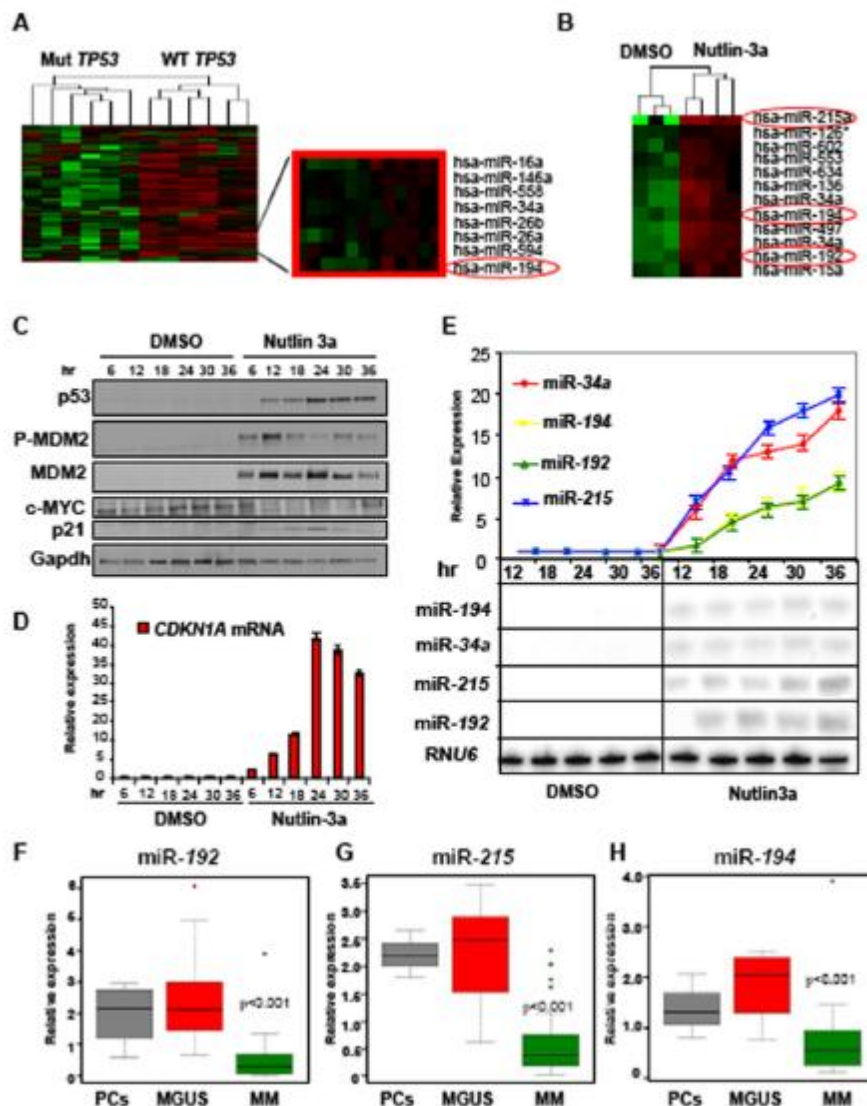
Results

Identification of p53-regulated miRNAs in MM

To determine if miRNAs are regulated by p53 in MM cells, we performed custom microarray analysis with an expanded set of probes capable of assaying the expression of more than 500 human miRNAs. Two approaches to compare the effect of p53 level on miRNA expression were used. We first assessed a specific signature associated with the presence of WT *TP53* in MM cell lines as shown in Figure 1A and Table S1. Six MM cell lines were used in the analyses: MM1s, NCI-H929 and KMS28BM which retain and express WT *TP53*; RPMI-8226, U266 with mutant *TP53*; and JJN3 that do not express *TP53* mRNA. Western blot analysis of these cells shows their p53 and MDM2 steady-state protein levels respectively (Figure S1A). Genomic and cDNA sequence analyses confirmed the presence of WT *TP53* cells in association with higher *MDM2* mRNA expression (Figure S1B). Several differentially expressed-miRNAs were identified (Table S1). Some of these miRNAs, such as those of miR-34 family, have been found to be associated with p53 status in other human malignancies (Hermeking et al., 2010). In the second approach, we performed miRNA microarray analysis in MM1s cells treated with or without Nutlin-3a (10 μ M), a small-molecule inhibitor of MDM2 (Figure 1B). In response to Nutlin-3a treatment, we identified expression of distinct miRNAs associated with p53 activation (Figure 1B. Table S2). Only two miRNAs were up-regulated in both analyses: miR-34a and miR-194 (Figure 1A, B; Table S1, S2). These results not only confirm up-regulation of miR-34a as a function of wild-type (WT) p53 status (He et al., 2007) but also point to strong up-regulation of miR-194 by p53 (Table S1, S2; Figure 1A,B). The significant up-regulation of miR-192 and miR-215 after p53 re-expression through Nutlin-3a treatment is especially interesting because they are located, together with miR-194, in two related microRNA clusters, the miR-194-2-192 cluster at 11q13.1 and the miR-215-194-1 cluster at 1q41.1

(Table S2), and have the same seed sequence. Genomic locations of these two clusters have been reported to be important for MM (Fonseca et al., 2009). miR-194 also has the same mature sequence regardless its expression cluster and miRNAs of the same cluster are usually expressed together (Garofalo et al., 2009; Ventura et al., 2008).

Figure 1



Identification of p53-regulated miRNAs in MM cells

p53 induces the expression of miR-192, 194 and 215

To confirm the microarray data, we first tested by q-RT-PCR for the presence of miR-34a, miR-194 and its cluster associate, miR-192 and 215, in WT TP53 compared to Mut TP53 cells (Figure S1C). WT TP53 cells retained higher expression of miR-34a, miR-194 and miR-192 (Figure S1C), but did not show expression of miR-215, suggesting that the 11q13.1 miR-194-2-192 cluster is associated with WT TP53 status in MM cells.

To determine the kinetics of p53 activation, we treated MM 1s cells with 10 μ M Nutlin-3a for different duration of time. p53 was barely detectable by immunoblotting at 6hr but increased after 12, 18 and 24 hrs of treatment and remain constant at 30-36 hrs (Figure 1C). The induction of p53 was also associated with MDM2 accumulation, p21 expression and c-MYC down regulation after 12 hrs of treatment (Figure 1C). The expression of p21-encoding *CDKN1A*, a p53 target gene, was also assessed by RT-PCR (Figure 1D). By northern blot and qRT-PCR analysis, we also studied the kinetics of miRNA activation during p53 up-modulation in MM 1s cells. The kinetics of miR-34a, miR-194, miR-192 and miR-215 expression (Figure 1E) were directly correlated with p53 protein up-regulation and p21 activation (Figure 1C,D), while for miR-15 and miR-29a/b the dynamics of expression appeared more related to down-regulation of their repressor c-MYC as expected (Chang et al., 2008) (Figure S1D,S1E, Figure 1D), than to p53 activation. To confirm the responsiveness of these miRNAs to p53, cell lines with varying *TP53* status were treated with Nutlin-3a or vehicle (DMSO), followed by qRT-PCR to monitor miRNA levels upon p53 activation (Figure S1F-S1K). Induction of miR-34a, miR-192, miR-215 and miR-194 was detected only in the cell lines treated with Nutlin-3a and harboring WT *TP53* ($p < 0.001$, Figure S1). Next, we analyzed induction of these miRNAs, by Nutlin-3a in freshly isolated CD-138+ PCs (Figure S1L), from 8 bone marrow aspirates of MM patients. Two samples (Pt-1 and Pt-2) exhibited *TP53* deletion by FISH analysis, while 6 (Pt-3 to Pt-8) retained *TP53* genes (Table S3). We detected induction of p53, miR-34a, 192, 194, 215 after 12 hrs of Nutlin-3a treatment (Figure S1M-S1O) in *TP53* WT samples, in association with different levels of *CDKN1A* mRNA activation (Figure S1O). Furthermore, to determine if these miRNAs are relevant in MM pathogenesis, we analyzed the expression of miR-194, 192 and 215 in a panel of CD138+ PCs obtained from newly diagnosed MM patients (n=33), MGUS (n=14) patients and normal donors (n=4) (Table S3) by qRT-PCR (Figure 1F-1H). Through Kruskal-Wallis analysis we found that these clusters of miRNAs are consistently down-regulated in MM samples ($p < 0.001$) compared to MGUS samples.

Identification of the p53 core element in the pri-miR-192-194-2 promoter at 11q13.1

To determine if p53 is directly involved in the transcriptional regulation of miR-194-2-192 and miR-215-194-1 clusters, we analyzed the cluster promoter regions. The upstream genomic region close to the transcription start site (TSS) (+1) (Hino et al., 2008) of pri-miR-194-2-192 contains several highly conserved regions among human, mouse, rat, and dog sequences (from -162 to +21 with respect to the TSS). To identify the promoter region responsive to p53 re-expression, we constructed reporter plasmids carrying various genomic sequences around the TSS of the pri-miR-194-2-192 cluster and subjected them to luciferase assay (Figure 2A). Bioinformatics search identified a previously reported high score p53 consensus site between -900/-912 bp (Sinha et al., 2008; Song et al., 2008), however this site was not functional for p53 activation since luciferase reporter constructs excluding this region retained full activity (P3-P7) (Figure 2A). The region from -245 to +186 bp (P7) had promoter activity comparable to that of the longest regions in MM cells after forced expression of p53 (Figure 2A), but regions from -125 to +186 bp (P8) and -912 to -245 bp (P10) did not. We identified a p53-responsive element between -245 and -125 bp (Figure 2B) because the construct excluding this region was not affected by p53 expression (Figure 2A). Since conserved regions in a given gene promoter are expected to contain regulatory elements, we focused on the highly conserved region controlling luciferase activity, the region between -161 and -135 bp. Luciferase assay using a construct mutated for each C and G contained in the two decamers of the hypothetical El-Deiry consensus sequence revealed that this non predicted and previously unpublished region is critical for p53 transcriptional activation of the pri-miR-194-2-192 cluster (Figure 2B). Indeed, we found that endogenous p53 directly interacts with the core element of the pri-miR-194-2 promoter in MM1s cells, as demonstrated by CHIP assay after 12 hr of Nutlin-3a treatment (Figure 2C). As a positive control, we used the p53 consensus site on the miR-34a promoter, while a nonspecific sequence served as

negative control (Figure 2C). Ectopic-expression of p53 activated the promoter of both members of the *miR-194-2-192* cluster in MM1s cells (Figure 2D). *MDM2* siRNA after p53 re-expression in MM1s cells led to higher relative luciferase activity and thus confirmed its dependence on p53 re-activation. Taken together, these data suggest that p53 is a key transcriptional activator of *miR-194-2* through directly binding to the core promoter element (Figure 2D). We also attempted to identify the promoter and primary transcript of *miR-215-194-1* on chromosome 1q41.1, but could not identify the primary transcript initiation point by 3' and 5' RACE and PCR amplification of the putative transcribed sequences (EST), however we confirmed the previously published consensus site for p53 by CHIP analysis (Figure S2).

Figure 2

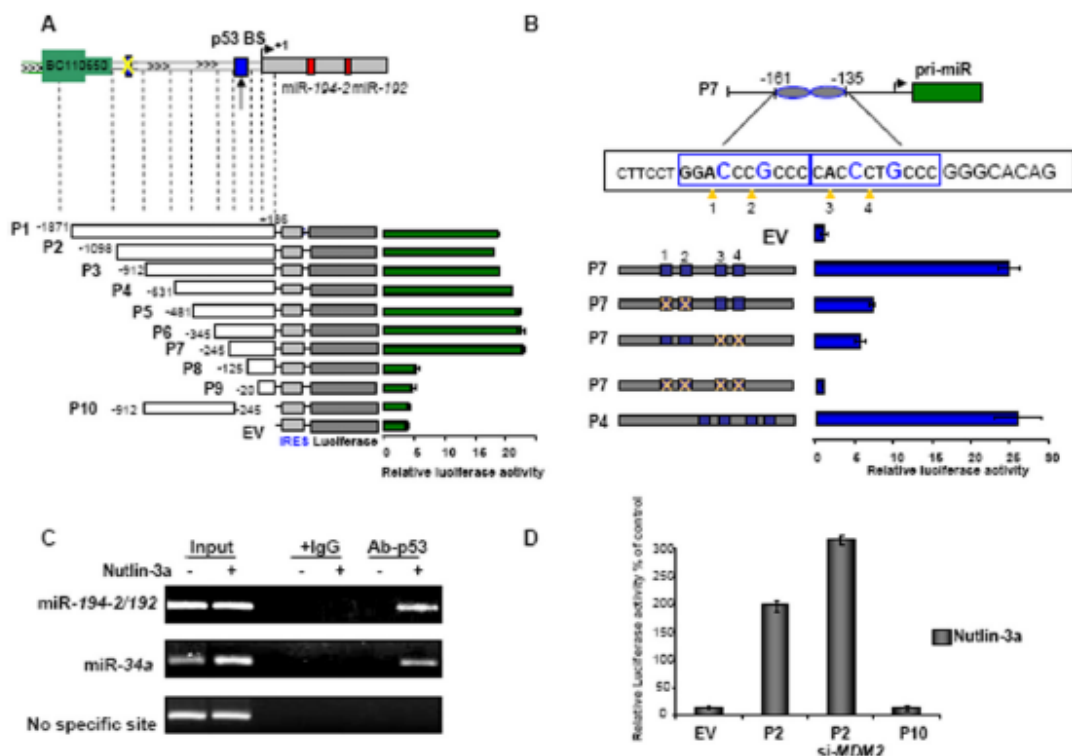


Figure 2. *miR-194-2-192* cluster is induced following p53 activation

A) Luciferase reporter activity of promoter constructs of *miR-192-194-2* cluster on chromosome 11q13.1 in MM1s cells after p53 transfection \pm SD. The arrow above construct P1 indicates the position of the transcription start site +1. p53 binding sites (BS) are indicated (blue box). **B)** Relative luciferase activity of P7 reporter construct. The magnified sequence highlighted in blue shows the location of the El Deiry p53 consensus binding sites in P7 construct sequence. Deletions introduced into the P7 construct are shown in yellow (X) showing abolition of the promoter activity. **C)** Chip assay after 24 hr of p53 non genotoxic activation, showing binding of p53 to the *miR-192-194-2* cluster promoter *in vivo* in MM1s cells. **D)** Luciferase activity of empty vector (EV), P2 and P10 reporter constructs after non genotoxic activation of p53 and *MDM2* mRNA silencing. Luciferase activities were normalized by Renilla luciferase activities. Values represent mean \pm SD from three experiments. See also figure S2.

miR-194-2-192 cluster is induced following p53 activation

miR-192, 194 and 215 affect p53-dependent MM cell growth

To examine the relevance of p53-mediated regulation of miR-192, 194 and 215 in MM, we first tested whether reintroduction of these miRNAs affected the biology of MM cells. Previous studies (Georges et al., 2008; Braun et al., 2008) showed that such reintroduction induced expression of p21 in different cancer cell lines which carried WT *TP53*, with a consistent G0/G1 arrest and p53 protein expression. The molecular mechanism of p53 re-expression remained elusive. To confirm this effect in our model, miR-192, miR-194 and miR-215 were introduced into transfection in WT *TP53* cell lines (MM1s, NCI-H929 and KMS28BM), as well as cells with mutated *TP53* (RPMI-8226), followed by detection of *TP53* and mRNAs of target genes *CDKN1A* and *MDM2*, by RT-PCR analysis (Figure S3). We found consistent re-expression of *CDKN1A* in *TP53* WT cells (Figure S3A) after transfection, but did not detect any increase in *TP53* mRNA (Figure S3B). Using MTS assay, we observed significant growth arrest in the cells transfected with miR-192, 215 and a less significant arrest with miR-194 in MM cells carrying WT *TP53* (Figure 3A-3C), as compared to scrambled sequences. By contrast, we did not detect this effect in RPMI-8226 cells (Figure 3D) expressing mutant *TP53*. Next, we determined if p53-responsive miRNAs interfere with the clonogenic survival of MM cells. MM cells were lentivirustransduced with miR-192, miR-215, miR-194 and miR-34a, miR-192 and 215 in WT p53 cells suppressed colony formation to an extent comparable to miR-34a, which was used as an internal control. Of note, miR-194 was less effective than miR-215 and miR-192. These miRNAs did not suppress colony formation in RPMI-8226 (Figure 3E and 3F) or U266 cells (unpublished data), while miR-34a did exhibit colony suppression in these mutant *TP53* cells, confirming its p53 independent apoptotic action (Hermeking et al., 2010).

Figure 3

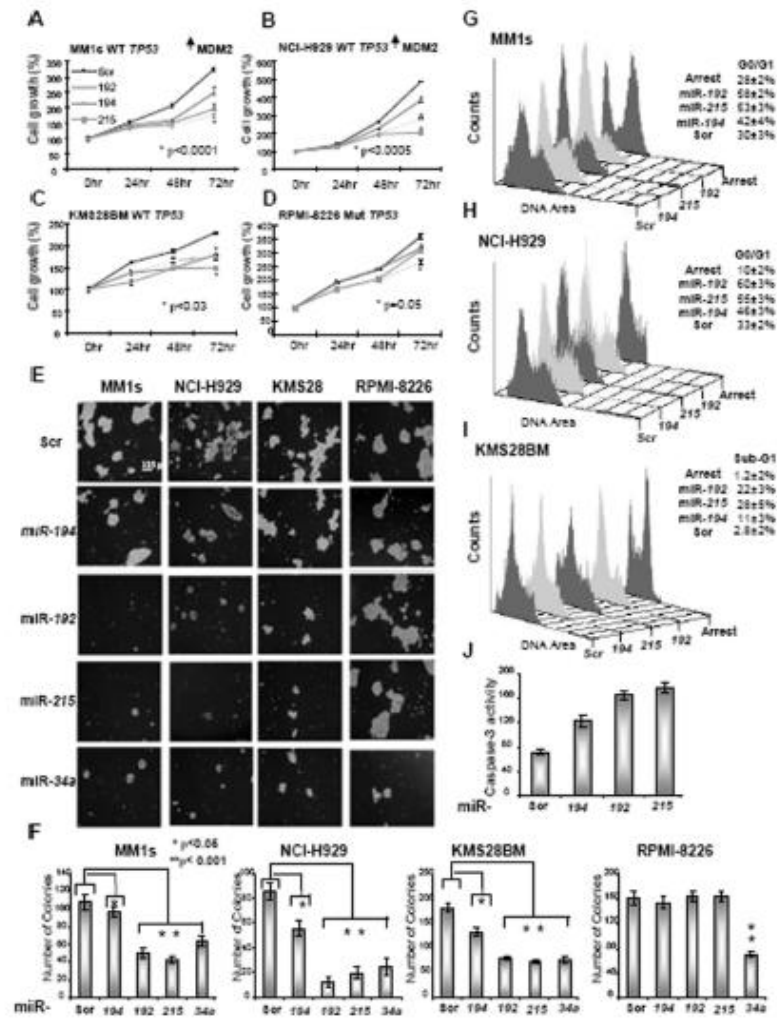


Figure 3. miR-192-194-215 induce decrease of proliferation and cell cycle arrest in WT TP53 MM cells

MTS assay performed in MM1s (A), NCI-929 (B), KMS28BM (C) and RPMI-8226 (D) cell lines. Cells were transfected with miR-192, 194, 215 and scrambled sequence (Scr) and were harvested at 24, 48, and 72 hrs after transfection. p values are indicated. See also figure S3. E,F) Soft agar colony suppression assay in WT TP53 and mutant TP53 MM cell lines after miRNAs transduction by lentivectors. Flow cytometry analysis in MM 1s (G), NCI-H929 (H) and KMS28BM (I) cells (miR-192, 194, 215 and Scr transfected) at 48 hr of transfection, after first being arrested and synchronized in G2/M phase by Nocodazole for 16 hr. Apoptosis in KMS28BM was evaluated by caspase-3 activity (J). All experiments were performed in triplicate \pm SD.

miR-192-194-215 induce decrease of proliferation and cell cycle arrest in WT TP53 MM cells

To further explore the p53-dependent mechanism(s) of miR-192, 215 and 194 interferences with cell growth and colony formation, we used flow cytometry to determine if their expression affects progression through the cell cycle. We noted that in the two WT TP53 cell lines with high expression of MDM2 mRNA, MM1s and NCI-H929 (Figure S1B), the p53-responsive miRNAs induced a consistent G0/G1 arrest. This

effect was observed in ~30% of scrambled-transfected cells vs ~60% of the cells transfected with miR-192 and 215 and ~45% for miR-194 (Figure 3G,H). By contrast in KMS-28BM cells, retaining WT *TP53* but expressing lower levels of *MDM2* mRNA (Figure S1B), we detected increases of sub-G₁ fractions (indicative of cell death) in cells transfected with miR-192 (~25% sub-G₁), 215 (30%) and 194 (12%) at 48 hrs after transfection, compared to ~3% in control cells transfected with the Scr sequence (Figure 3I). At 48 hrs after transfection we also detected increased caspase-3 activity (Figure 3J). The differential effect of the miRNAs on *TP53* WT cells carrying lower *MDM2* mRNA basal expression (Figure S1B) led us to analyze *MDM2* levels after miRNA transfection (Figure S3C). *MDM2* mRNA, but not protein, was detected after MM cells transfection. Because *MDM2* protein is rapidly auto-ubiquitinated and degraded through the proteasome pathway (Marine et al., 2010); p53 induction is necessary for its detection in MM cells (Stuhmer et al., 2006; Ooi et al., 2009). Only in one (Mut *TP53* RPMI-8226) of six MM cell lines analyzed, was *MDM2* protein detected without p53 activation (Figure S1A, S1G). We also noted that *MDM2* mRNA was down-regulated after ectopic expression of these miRNAs, mostly in WT *TP53* cells, but to some extent also in Mut *TP53* cells (RPMI-8226) (Figure S3C). These data were confirmed at the protein level in RPMI-8226 cells where we observed ~20% down regulation of *MDM2* protein at 72 hr after miRNA transfection (Figure S3D). The results indicate that ectopic expression of miR-192, 215 and 194 in WT *TP53* cells inhibits cell growth and enhances apoptosis, effects that could be related to *MDM2* regulation in MM cells.

Human *MDM2* is a direct target of miR-192, 194 and 215

The data thus far demonstrate that the biological functions of miR-192, 215 and 194 in MM cells is p53-dependent. After introduction of these miRNAs the *TP53* mRNA level did not change in MM cells but higher *CDKN1A* and lower *MDM2* mRNA levels were observed (Figure S3). Both genes, *MDM2* and *CDKN1A*, are direct targets of p53 but their expression in this case was not preceded by *TP53* transcription (Figure S3B). Thus, we hypothesized that miR-192, 194 and 215 could target the expression of *MDM2*. To further examine the effects of these miRNAs on *MDM2* protein expression in WT *TP53* MM cells, we analyzed the consequences of ectopic expression of miR-192, miR-194 and miR-215 at 72 hrs after transfection and 12 hrs of non genotoxic activation of p53 by Nutlin-3a (10 μ M). Increased expression of these miRs upon transfection was confirmed by qRT-PCR (Figure S4A), and the effects on p53, *MDM2* and p21 levels were analyzed by Western blot (Figure 4A). Over-expression of miR-192, 194 and miR-215 significantly increased the level of p53 and p21 at 12 hrs after Nutlin-3a treatment compared to Scr-transfected cells ($p < 0.001$), as shown by densitometric analysis in Figure 4B,C. Expression of *MDM2* protein was dramatically decreased in both cell lines (Figure 4A-C). Conversely, knockdown by 2'-O-me-anti-miR-192-194 and 215 (pool) after 12 hr of Nutlin-3a treatment, as confirmed by qRT-PCR (Figure S4B) in *TP53* WT cell lines, increased the level of *MDM2* protein ($p < 0.01$), while p21 and p53 protein levels were attenuated ($p < 0.01$) (Figure 4B), as confirmed by densitometry (Figure 4E). We also confirmed that *MDM2* mRNA levels were strongly reduced in the miR-192, 194 and 215 transfected cells at 6 and 12 hr of Nutlin-3a treatment in both cell lines (Figures 4C). These results indicate that miR-192, 194 and 215 induce the degradation of *MDM2* mRNA, confirming that they regulate both, protein and RNA levels. We next tested whether *MDM2* is a direct target of these miRNAs by performing a bioinformatics search (Target Scan [Lewis et al., 2003], Pictar [Krek et al., 2005]), but were unable to identify the 3'-UTR of *MDM2* as a target. Because the 3'-UTR of *MDM2* is not well conserved across species, we decided to use the RNA22 target prediction program (Miranda et al., 2006) which does not need validated targets for training, and neither requires nor relies on cross-species conservation. RNA22 predicted two miRNA responsive elements (MREs) for miR-192/215 and two MREs for miR-194 in the 3'UTR of human *MDM2* (*HDM2*) (Figures 4D and S4C-S4G). To verify that *HDM2* is a direct target of miR-192, miR-194 and miR-215, *HDM2* 3'UTR containing all MREs (~4K), was cloned into pGL3 basic construct downstream of the luciferase open reading frame (Figure 4D). This reporter construct was

used to transfect MM1s cells which express the endogenous miRs following up-modulated p53 expression. Increased expression of these miRs upon transfection significantly diminished luciferase expression (Figure 4D). We subsequently screened the predicted MREs on the 3'UTR of *HDM2* mRNA, using luciferase assays with 4 different constructs carrying the MREs for miR-192/215 and miR-194 (Figure S4H-S4K). We observed that expression of each specific MRE reporter construct was specifically down regulated upon transfection of each individual miRNA. Conversely, when we performed luciferase assays using a plasmid harboring the binding sites inactivated by site-directed mutagenesis, we observed a consistent reduction in the inhibitory effects (Figure S4H-S4K). We also analyzed the expression of *MDM2* mRNA in a panel of CD138+ PCs obtained from MM patients, MGUS patients and normal donors by RT-PCR (Figure 4E). Through Kruskal-Wallis analysis we found that *MDM2* mRNA is significantly up-regulated in MM samples ($p < 0.001$) compared to MGUS samples and normal PCs (Figure 4E). Using non parametric test analysis, we found a significant inverse correlation between miR-192 expression and *MDM2* mRNA in MM samples (Sperman $\rho = -0.698$, $p < 0.001$, $n = 33$) (Figure 4F).

Figure 4

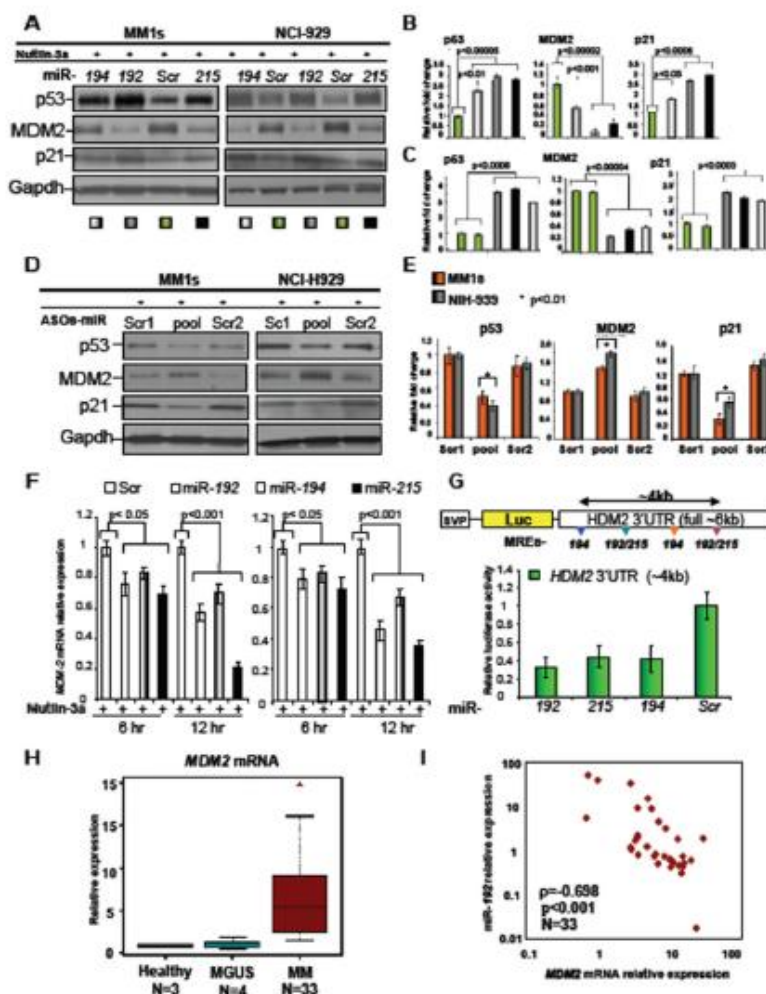


Figure 4. miRNA-192-194 and 215 effect on MDM2 protein and mRNA levels

miRNA-192-194 and 215 effect on MDM2 protein and mRNA levels

miR-192, 194 and 215 re-expression enhances sensitivity of WT TP53 MM cells to non genotoxic activation of p53 *in vitro* and *in vivo*

To determine if re-expression of the miRNAs could enhance sensitivity of WT TP53 MM cells to non genotoxic activation of p53, we tested MI-219, a highly selective, orally active small-molecule inhibitor of the MDM2-p53 interaction (Shangary et al., 2008). We first examined whether MI-219 induces p53, MDM2, p21 and Puma up-regulation in MM1s cells after miR-192, miR-194 and miR-215 transfection. In cells with forced expression of miR-192 and 215, p53 became detectable even in untreated cells (Figure 5A-5B) ($p < 0.05$), confirming previously published data in other cell lines (Georges et al., 2008; Braun et al., 2008). p53 re-expression and subsequent p21 and Puma up-regulation was observed in these cells and in miR-194 transfected cells, and is clearly visible following 24 hrs of 2.5 μM MI-219 treatment (Figure 5A). In control cells (Scr) the treatment was ineffective (Figure 5A). Densitometric analysis of p53 and MDM2 protein levels was performed when cells were treated for 24 hr with 2.5 μM , 5 μM and 10 μM MI-219 (Figure 5B). Confirming our previous data, we observed higher p53 accumulation (≥ 2 -fold increase, $p < 0.001$) and dramatic MDM2 down-regulation (≥ 3 -fold decrease, $p < 0.001$) in miRNA transfected cells (Figure 5B). These opposing changes in MDM2 and p53 expression levels correlated with higher activation of p53 downstream targets, p21 and Puma (Figure 5A). Furthermore, MI-219 induced higher caspase-3 activation in the presence of miR-192, miR-194 and miR-215 ($p < 0.001$) (Figure 5C). Next, we examined whether activation of p53 by MI-219 leads to apoptosis in MM cells. Indeed, treatment with MI-219 induced apoptosis as revealed by Annexin V staining (Figure 5D). In cells transfected with a pool of miRNAs MI-219 effectively ($p < 0.0002$) induced apoptosis at 2.5 μM ($27 \pm 3\%$), 5 μM ($32 \pm 3\%$) while the scrambled control did not. This effect was less significant when using MI-219 at 10 μM ($30 \pm 5\%$), though it was enhanced when treatment was combined with miRNAs ($55 \pm 5\%$) (Figure 5D). Increased concentration of MI-219 did not increase the apoptotic rate of scrambled-transfected cells but caused non-specific toxicity (data not shown).

Figure 5

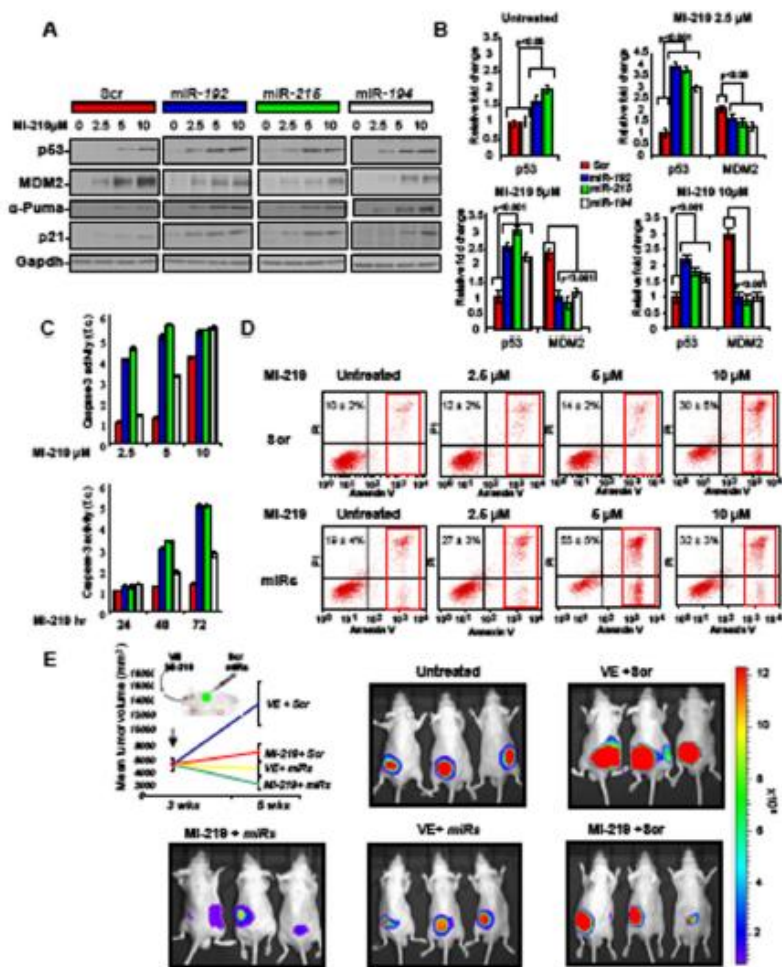


Figure 5. miR-192, 194 and 215 increase sensitivity to MI-219 *in vitro* and *in vivo* by targeting *MDM2*

A) Effects of miR-192, 194 and 215 on endogenous p53, p21 and MDM2 levels (Western blots) in MM1s cells treated with MI-219 at different concentrations. Densitometric analysis for p53 in untreated cells and for p53 and MDM2 protein levels in 2.5, 5 and 10 μ M MI-219-treated cells is reported (B) All experiments were performed in triplicate \pm SD. C) Apoptotic effect at different concentrations and time points for each miRNA transfected cells was assessed by caspase-3 activation assay \pm SD. D) Apoptosis associated with the pool of these miRNAs upon MI-219 treatment (24 h) at different concentration (2.5-10 μ M) was evaluated by Annexin V. All experiments were performed in triplicate \pm SD. E) Gfp/Luc + MM1s cells were injected subcutaneously into the flanks of nude mice; at 3 wk post-injection, mice with comparable tumor sizes were selected for treatment (untreated). *In vivo* confocal imaging of GFP+/Luc+ MM cells engrafted in athymic nu/nu mice after 2 wk of combined treatment with oral MI-219 or Vehicle (VE) plus pre-microRNA pool or Scr sequence directly into the tumors. Graphic represents the mean of tumors value (mm²) before (3 wk) and after the treatment (3+2 wk) \pm SD.

miR-192, 194 and 215 increase sensitivity to MI-219 *in vitro* and *in vivo* by targeting *MDM2*

Because previous studies have shown that MI-219 achieved excellent oral availability, we investigated if, in mouse xenograft models, the combined action of miRNAs and oral MI-219 could suppress tumorigenicity of MM cells. 8×10^6 viable MM1s Gfp+/Luc+ cells were injected subcutaneously into the right flank of 40 nude

mice. At 3 wks after injection a group of 32 mice with comparable tumor size were selected and randomly divided into 4 groups for 4 independent experiments, using 8 mice for each combined treatment (Figure 5E). Specifically, we used the combination of oral treatment with 200 mg/kg MI-219 or vehicle control (VE) once a day for 14 days plus direct tumor injection of double strand RNA scrambled sequence (Scr) or a pool of pre-miR-192, 194 and 215 (miRs). Whereas the VE-Scr treated tumors increased 2-fold in volume in 2 wks (from $5390 \pm 993 \text{ mm}^3$ to $13500 \pm 3200 \text{ mm}^3$ [$p < 0.0001$]), MI-219/Scr-treated tumors remained static in volume ($5390 \pm 993 \text{ mm}^3$ to $5400 \pm 1200 \text{ mm}^3$) (Figure 5E). By contrast, mice treated with VE-miRs showed ~1.5-fold reduction in tumor size (from $5390 \pm 993 \text{ mm}^3$ to $3700 \pm 950 \text{ mm}^3$ [$p < 0.01$]). The most effective combination was MI-219 plus miRs, where mice showed 5-fold reduced tumor volumes (from $5390 \pm 993 \text{ mm}^3$ to $2100 \pm 560 \text{ mm}^3$ [$p < 0.01$]) and >93% reduction when compared to VE/Scr treatment (Figure 5E). These findings demonstrate proof-of-concept for *in vivo* therapy of MM using combined miRNAs and an MDM2 pharmacological inhibitor.

miR-192 and miR-215, by antagonizing MDM2 down-regulation, target IGF-1 and IGF1-R

Since our data demonstrate that miR-192, miR-194 and miR-215 target *MDM2*, we sought to determine if MDM2 substrates could also be affected. IGF-1R is a known target of MDM2 ubiquitin ligase function (Girnita et al., 2003; Froment et al., 2008). Therefore, by targeting *MDM2*, miR-192, 194 and 215 may indirectly influence the expression of IGF-1R. In MM cells, IGF-1R and its ligand, IGF-1, are key factors in regulation of PC migration into the bone marrow (Qiang et al., 2004; Tai et al., 2003). We noted that in WT *TP53* MM cells, p53 re-expression was strongly associated with down-regulation of IGF-1R and IGF-1 (Figure S5A and S5B) compared to mutant *TP53* MM cells (Figures S5C and S5D). We sought to determine the effect of miRNAs on IGF-1R and IGF-1 expression through targeting MDM2. We found that in the presence of miR-192, 215 but not *miR-194*, IGF-1R and IGF-1 protein levels decreased, as determined by Western blot analysis (Figure 6A).

Figure 6

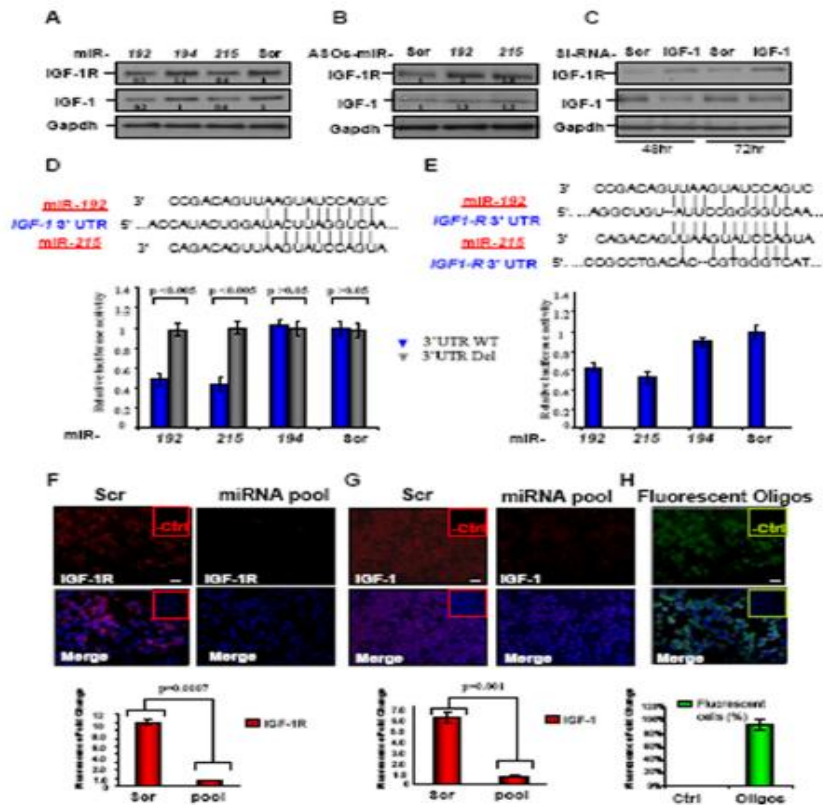


Figure 6. miR-192-215 regulate IGF-1 and IGF1-R expression in MM cells
 Western blot showing IGF-1R and IGF-1 expression after miR-192 and miR-215 transfection using pre (A) and ASOs (B) for miR-192, 215, 194 and Scr in MM1s cells treated for 12 hr with Nutlin-3a. Densitometric analysis is reported. See also figure S5. C) Western blots after IGF-1 knockdown in MM1s (si-RNA) using anti-IGF-1R, IGF-1 and Gapdh antibodies. D-E) miRNAs predicted to interact with *IGF-1* and *IGF-1R* gene at their 3'-UTR, according to "in silico" Target Scan (*IGF-1*) and RNA-22 (*IGF-1R*) prediction software (see also figure S5). Luciferase assay showing decreased luciferase activity in MM 1s cells co-transfected with pGL3-*IGF-1*-3' UTR (D) or pGL3-*IGF-1R*-3' UTR (full) (E) and miR-192, 194, 215 or Scr. Deletion of 6 bases in all putative consensus sequences on *IGF-1*-3' UTR abrogates these effect (Del) (D). See also Figure S5. Bars indicate relative luciferase activity \pm SD. All experiments were performed in triplicate. F-G) Immunofluorescence using anti-IGF-1R (F) and anti-IGF-1 (G) in red and blue nuclear DNA, from CD-138+ PCs from 9 MM patients transfected with miR-192 and miR-215 (pool) or Scr and intensity of the signal was assessed \pm SD. The efficiency of the transfection in the 9 samples was evaluated using fluorescent double strand RNA oligos (H). Scale bars indicate 25 μ M.

miR-192-215 regulate IGF-1 and IGF1-R expression in MM cells

Furthermore, inhibition of endogenous miR-192/215, using antisense oligonucleotides, combined with 24 hrs of Nutlin-3a treatments increased both IGF-1R and IGF-1 levels in MM1s cells (Figure 6B). This effect was not seen with miR-194. To determine if the regulation of IGF-1 does affect IGF1R in MM cells, we silenced IGF-1 and observed up-regulation of IGF-1R protein levels at 48 and 72 hrs post treatment (Figure 6C). This effect was clearly different from that observed following miRNA transfection (Figure 6A). We next

tested whether miR-192 and 215 target IGF-1R and IGF-1 directly by generating luciferase reporters containing their 3' UTRs. Using Targetscan (Lewin et al., 2003) Pictar (Krek et al., 2005) and RNA22 (Miranda et al., 2006) searches we, identified several MREs for miR-192 and miR-215 but not for miR-194 in the 3'UTR of *IGF-1R* and *IGF-1* mRNAs (Figures 6D,E). Luciferase activity dropped 40–50% when these constructs were co-transfected into MM1s cells with miR-192, 215 compared to miR-194 and Scr (Figures 6D, 6E, S5E-S5I). To determine if in freshly isolated CD-138+ PCs these miRNAs could regulate IGF-1 and IGF-1R expression, we transfected miR-192 and 215 (pool) into PCs of 9 patients and we performed immunofluorescence analysis for IGF-1R and IGF-1 at 48 hrs. We observed a significant decrease in IGF-1R and IGF-1 protein expression (Figures 6F,G). Transfection efficiency was confirmed using RNA Fluorescent Oligo (Figure 6H). These results indicate that miR-192 and miR-215 directly target *IGF-1R* and *IGF-1* in MM.

miR-192 and 215 block MM migration and invasion *in vitro* and *in vivo*

Given the known role of IGF-I and IGF-1R as anti-apoptotic factors and in MM migration through endothelial barriers and bone marrow stroma (Qiang et al., 2004; Tai et al., 2003), we sought to determine if miR-192 and 215 interfere with the chemotactic function of IGF-I and block migration and invasion of MM cells. We first determined that miR-192 and 215 actions on the IGF-1 axis in MM affect both WT *TP53* (MM1s) and mutant (RPMI-8226) cell lines (Figure 7A) and that the down-regulation of both proteins critically affects S6 and AKT phosphorylation in these cells. Next, we found that ectopic expression of miR-192 and 215 in NCI-H929 and RPMI-8226 IGF-1 treated cells was associated with significant decrease in cell adhesion (Figure S6A,B), migration and tissue invasion compared to Scr control. To this end, we used an intra-epithelial trans-well migration assay with IGF-1 at various concentrations as attractant and two bone marrow-derived stromal cells, HS-5 (fibroblastlike) and HS-27A (epithelial-like) as cell layer. As shown in Figures 7B and S6C, IGF-1 (50 ng/ml) stimulated migration of MM cells, MM1s and RPMI-8226. To further examine the role of miRNA-192, 215 and 194 in MM cells, we investigated the effect of these miRNAs on migration *in vivo*, using a previously described homing model (Roccaro et al., 2008). Nine NOD-SCID mice (for each group) were intravenously injected with 8×10^6 of pre-miRNA-192-, 194 and 215 or Scr probe-transfected GFP⁺/Luc⁺MM1S cells. One week later, mice were injected intravenously every week for 4 weeks with an individual miRNA or Scr dissolved in PBS (10 µg for each mouse). After 5 wks the homed and proliferated tumors were markedly suppressed in miRNA-treated mice compared to Scr-transfected MM cells ($p < 0.01$) (Figure 7C). At 5 wks post-injection we first noted reduced tumor progression, by bioluminescence imaging (Figure 7D). Mice injected with Scr-transfected MM1s in addition to serial iv-injection with Scr showed significant tumor growth, but tumor burden was significantly reduced in mice injected with pre-miR-194 and was nearly nonexistent in mice injected with either pre-miR192 or pre-miR-215 (Figure 7C,D). In addition, through FACS analysis using human CD-138+ antibody we analyzed bone marrow engraftment of these cells in injected NOD-SCID mice. We confirmed that Scr-treated mice showed bone marrow engraftment of $\sim 25 \pm 15\%$ of MM1s cells vs $4 \pm 2\%$ for miR-192 and $2 \pm 2\%$ for miR-215 animals (Figure 7E). The *in vivo* action of miR-194 was less effective, $12 \pm 3\%$ of bone marrow engraftment MM1s cells compared to miR-192 and 215 but still higher than the Scr control (Figure 7E). These data indicate that miR-192, 215 but also miR-194 have therapeutic potential not only by affecting proliferation rates in MM cells but also by affecting the homing and migration ability of MM cells.

Figure 7

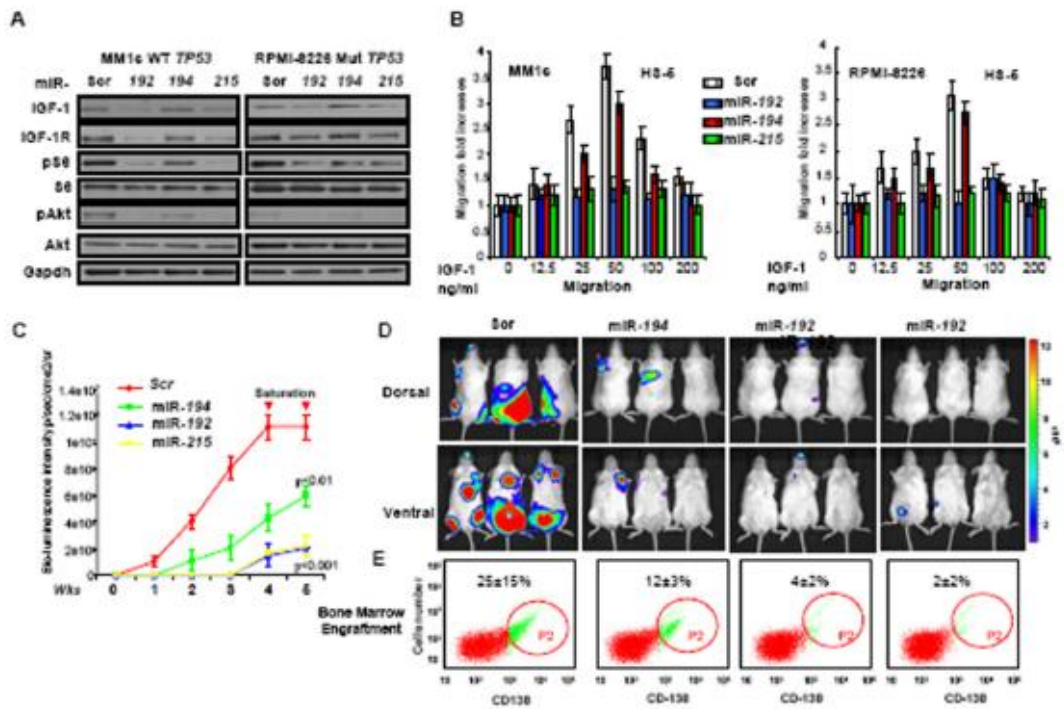


Figure 7. miR-194, 215 and 194 block invasion ability of MM cells

A) MM1s and RPMI-8226 cells (pre-miRNA-192, 194, 215, Scr-transfected) were harvested 72 hr after transfection. Whole cell lysates were immunoblotted using IGF-1, IGF-1 R, pS6, S6, p-Akt, Akt and Gapdh antibodies; Scr sequence and miR-194 transfected cells served as controls. The experiments were performed in triplicate. B) Intra-epithelial migration assay in MM cells miRNAs transfected using HS-5 cells at different concentrations of IGF-1 as attractant. Bars indicate relative fold change of migration compared with the control \pm SD. See also figure S6. C-D) *In vivo* confocal imaging. 8×10^6 GFP+/Luc+ MM1s cells were transfected using either pre-miRNA-192, -194, 215 and Scr RNA oligos and then iv injected into mice immediately after transfection. After 1 wk the mice were miRNAs iv injected (10ug) once a wk for 4 wk and the bioluminescence intensity was assessed before every injection (C). (D) Representative bioluminescence imaging (BLI) after 5 wk from the injection. (E) Bone marrow cells from the mice used for the experiment were isolated and human CD-138 positive cells (engrafted cells) were detected using anti-CD-138 antibody by flow cytometry (P2 fraction) (E).

miR-194, 215 and 194 block invasion ability of MM cells

Discussion

Complex cytogenetic abnormalities and numeric chromosomal aberrations occur in virtually all multiple myeloma, and in most, if not all, cases of MGUS (Kuehl and Bergsagel, 2002). Paradoxically, mutations and/or deletion of *TP53* occur in only a small percentage of intramedullary MMs and not at all in MGUS (Chng et al., 2007). Several reports (Teoh et al., 1997; Quesnel et al., 1994) and our data (Figure 4E) suggest

that MDM2 over-expression in MMs, but not its gene amplification (Quesnel et al., 1994), could be responsible for p53 inactivation in cells retaining functional p53 pathways. This supports the idea that induction of p53 in this setting might be a suitable treatment for MM. There have been a few reports concerning microRNA deregulation in MM and although not all reported findings were in agreement, they confirmed that such deregulation is important in MM pathogenesis (Pichiorri et al., 2008; Roccaro et al., 2009; Lionetti et al., 2009; Gutierrez et al., 2010). Here, we studied the role of miRNAs in the p53 apoptotic pathway upon non genotoxic activation of p53 in MM cells, using small molecular inhibitors of MDM2 (Nutlin-3a, MI-219). Upon p53 activation we identified two related microRNA clusters located in regions considered important for MM (miR-194-2-192 at 11q13.1 and miR-194-1-215 at 1q41.1) (Fonseca et al., 2009). Furthermore, the knowledge that miRNAs coming from the same cluster can reinforce their action on the same cellular pathways (Garofalo et al., 2009; Ventura et al., 2008), led us to study the molecular mechanisms associated with activation of the p53 pathway by these miRNAs. Through characterization of the miR-194-2-192 cluster promoter region and definition of a non canonical p53 consensus site we have shown that these miRNAs are direct p53 targets. In patient samples the expression of these miRNAs changed during transition from normal PC, *via* MGUS to intramedullary MM; these miRNAs were significantly down-regulated in a cohort of newly diagnosed MMs vs MGUS; miR-192, 215 and 194 enhanced colony suppression, cell cycle arrest or apoptosis in a p53-dependent manner. We also noted, as in the case of KMS28BM cells, that their biological action could be associated with the MDM2 status in MM cells. The short half-life of MDM2 protein (Marine et al., 2010) and difficulties in analyzing its protein expression in MM cells without p53 activation, led to the demonstration that the effect of these miRNAs on MDM2 was clearly detectable after treating WT *TP53* MM cells with combined Nutlin-3a and ectopic expression of the miRNAs. In fact, we observed that in treated cells with enforced expression of these miRNAs MDM2 was dramatically down-regulated at protein and mRNA levels and this down-regulation was inversely associated with higher p53 expression and p21 activation (Figure 4A-4C). Luciferase assays using plasmids harboring the *MDM2* 3-UTR sequence strongly confirmed that *MDM2* is the direct target of these miRNAs. In a subset of newly diagnosed MMs, elevated levels of *MDM2* mRNA were inversely associated with miR-192 expression. We proved, *in vivo* and *in vitro*, that the combination of these miRNAs with p53 pharmacological activator (MI-219), leading to MDM2 down-regulation and subsequent p53, p21 and Puma up-regulation, could be a successful therapeutic strategy. In fact it produced anti-tumor results that could not be achieved solely by increasing the drug concentration. We also found that miR-192 and miR-215 expression, by overriding MDM2 ubiquitination of IGF-1R (Girnita et al., 2003; Froment et al., 2008), directly targets the IGF-1 axis in MM cells, controlling mobility and invasive properties of MM cells *in vitro* and *in vivo*. We propose a model in which these miRNAs are: 1) regulators of the auto-regulatory loop, increasing the window of time between p53 apoptotic action and p53 degradation by MDM2; and 2) at the same time targeting the IGF axis, antagonizing the MDM2 ubiquitin ligase function on IGF-1R (Figure 8).

Figure 8

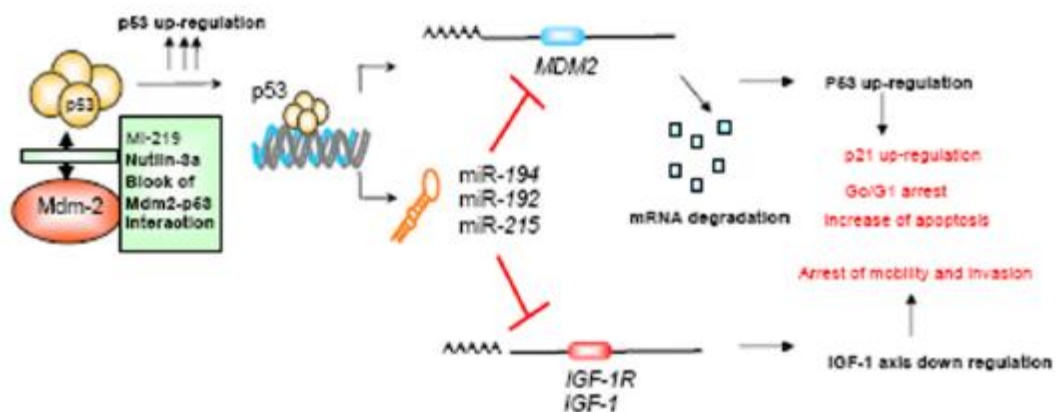


Figure 8. miR-192, 215 and 194 impair the p53/MDM2 auto-regulatory loop
Model to illustrate the possible role of miR-192, 194 and 215 in control of MDM2 and IGF-1/IGF-1R pathways in MM cells. See also figure S7.

miR-192, 215 and 194 impair the p53/MDM2 auto-regulatory loop

During Nutlin-3a treatment of primary CD-138+ PCs from MMs without *TP53* deletion, we noted that p21 activation, as well as re-expression of the three miRNAs, was consistent but not uniform in all samples analyzed. Possibly mechanisms other than alterations to the *TP53* gene could influence the sensitivity to MDM2 molecular inhibitors. In seeking an explanation for the lack of expression of these miRNAs in MMs, we noted that the genes for these miRNAs are located in chromosomal regions in MM that are normally characterized by chromosome gain and translocations rather than deletions (Fonseca et al., 2009). We then, explored the methylation status in the promoter of the miR-194-2-192 cluster. By combined bisulfite restriction analysis (COBRA) we detected hypermethylation of the promoter region of this cluster (Region R) (Figure S7A) in MM cell lines (Figure S7B). Furthermore, treatment of MM cell lines with a demethylation agent (Azacytidine) increased the expression of these miRNAs in WT *TP53* MM cell lines (Figure S7C). Re-expression of the *SOCS-1* gene, known to be silenced by hypermethylation in MM cells (Galm et al., 2002), served as internal control.

It is likely that the transition from MGUS to MM is favored by clonal selection of cells with aberrant promoter methylation of the miR-194-2-192 cluster. This could be associated with a decreasing ability of p53 to down-modulate MDM2 expression thus tipping the regulatory balance in favor of MDM2 in MM cells. This proposed model (illustrated in Figure S7D) will require further investigation.

Of note, monoallelic deletion of *TP53* in MM, which often seems to occur without mutation on the other allele, is associated with an extremely poor prognosis (Chng et al., 2007). This supports the idea that a two-fold decrease in *TP53* gene content is associated with tumor progression, which supports the hypothesis that a partial lack of expression of these miRNAs in MMs could create a p53 imbalance with direct biological consequences.

In summary, our results have defined a mechanism of p53 regulation through miRNAs acting on MDM2 expression, providing the basis for the development of miRNA-targeted therapies for MM, as illustrated in Figure 8.

Experimental Procedures

Collection of primary cells

33 newly diagnosed primary MM samples, 14 primary samples from monoclonal gammopathy of undetermined significance (MGUS), and 5 primary samples from healthy donors were obtained from bone marrow aspirates. Written informed consent was obtained in keeping with institutional policies (IRB-approved procurement protocol (2000C0247) at The Ohio State University and The University of Turin GIMEMA-MM-03-05, N. EUDRACT 2005-004745-33). Three of the five healthy PCs used were purchased from *AllCells* LLC. (Emeryville, CA).

Luciferase Assays

MM1s cells were cotransfected with 1 µg of pGL3 firefly luciferase reporter vector (see luciferase reporter vector method supplementary information), 0.1 µg of the phRL-SV40 control vector (Promega), and 100 nM miRNA precursors (Ambion) using nucleoporation (LONZA) Cell Line Nucleofector Kit V as previously described. Firefly and Renilla luciferase activities were measured consecutively by using the Dual Luciferase Assay (Promega) 24 hr after transfection. Each reporter plasmid was transfected at least twice (on different days) and each sample was assayed in triplicate.

Mouse experiments

Animal studies were performed according to institutional guidelines. 1×10^6 of GFP/Luc + MM1s cells were suspended in 0.10 ml of extracellular matrix gel (BD Biosciences) and the mixture was injected subcutaneously into the right flank athymic nu/nu mice. 3 wks after injection, mice with comparable size tumors were treated for 2 wks with a combination of oral dose of MI-219 (200 mg/kg) or vehicle, once a day for 14 days and miRNAs or scrambled sequence oligos (10ug) (Ambion), was injected directly into the tumors once a week for 2 wks. For the NOD-SCID engraftment model Luc+/GFP+ MM.1S cells (8×10^6 /mouse) were injected into the tail vein of SCID mice (. Treatment started 7 days from tumor cell inoculation, by weekly i.v. injections of miRNAs or scrambled sequence. RNA oligos (Ambion) (10 µg) for four cycles (4 wks total). For more details see in vivo experiments supplemental data.

Transfection method for primary cells and MM cell lines

CD-138+ PCs obtained from new diagnosed MM patients and isolated as previously described were transfected by using nucleoporation (LONZA) Cell Line Nucleofector Kit V (Cat#VCA-1003). MM1s, NCI-H929 cell lines were transfected by using using nucleoporation (LONZA) Cell Line Nucleofector Kit V (Cat#VCA-1003). Instead for U266, KMS-28BM and RPMI-8226 Cell Line Nucleofector Kit C (Cat#VCA-1004) was used. Specifically for primary cells 1×10^6 CD-138+ PCs were resuspended in 100 µl of V solution and 100 nM miRNA precursors (Ambion) was used for the transfection reaction. For more details see transfection method for primary cells supplemental information.

Target Screening

In this study, we used three publicly available search engines for target prediction to obtain the putative targets: TargetScan (Release 2.1), <http://genes.mit.edu/targetscan>, Pictar, <http://pictar.bio.nyu.edu> and Rna22, http://cbcsrv.watson.ibm.com/rna22_targets.html. For RNA22 predicted sites we considered only the heteroduplex with a folding energy > -27 Kcal/mol (Figures S8B-8E) because we were not able to

confirm by luciferase assay the interactions between target gene and miRNAs with a folding energy less than -27 Kcal/mol (data not shown).

Array data

Data deposition

The microarray data have been deposited in the Array Express database, www.ebi.ac.uk/arrayexpress (accession no. E-TABM-1037 and E-TABM-1038).

Supplementary Material

Figure S1. miR-34a, miR-194 and miR-192 expression are related to TP53 status in MM cells. (A-B) p53 and MDM2 expression in MM cell lines used for microarray experiments A) 80 µg of whole cell lysate of MM cell lines used for microarray experiments, were subjected to Western blot analysis using p53, MDM2 and Gapdh antibodies B) MDM2 mRNA levels in MM cell lines carrying WT TP53 compared to normal PCs (N=4). Relative expression of MDM2 mRNA in MM1s, NCI-H929 and KMS28BM cell lines compared to the average MDM2 mRNA expression of 4 normal PCs. The PCR products for the MDM2 gene were normalized to GAPDH mRNA expression. Values represent mean ± SD from three experiments. (C) miR-34a, miR-194 and miR-192 relative expression in WT TP53 (MM1s, NCI-H929, KMS28BM) and Mutant/Null TP53 cells (RPMI-8226; U266, JIN3) measured by q-RT-PCR. Bars represent relative fold changes, expressed in 2^{-ΔCT} values ±SD obtained from three independent experiments. RNU44 expression was used for normalization. (D) Kinetics of activation of miR-15a, 29a and 29b in MM 1s cells upon Nutlin-3a treatments, measured by qRT-PCR and Northern blot analysis. Lines represent relative fold changes, expressed in 2^{-ΔCT} values ±SD obtained from three independent experiments. RNU44 expression was used for normalization for the qRT-PCR experiments and RNU6 for the northern blot analysis. (E) Time course of MYC mRNA expression in Nutlin-3a treated MM 1s cells by RT-PCR. The PCR product was normalized to ACTIN mRNA expression. Values represent mean ± SD from three independent experiments. (F-K) miR-192, miR-194 and miR-215 re-expression is dependent on p53 activation. Western analysis for p53, MDM2 and Gapdh in NCI-H929 (WT TP53) (F), RPMI-8226 (Mut TP53) (G) and U266 (Mut TP53) (H) cell lines after different times of Nutlin-3a treatment. All experiments were performed in triplicate. Stem loop q-RT-PCR showing the time course of miR-192, 194, 215 and 34a expression in NCI-H929 (I) RPMI-8226 (J) and U266 (K) cells Nutlin-3a treated compared to DMSO treatment The PCR products were normalized to RNU6B expression. Bar-graphs represent mean values observed in four separate studies ± SD. L) Representative flow analysis of purified CD-138+ plasma cells with purity more than 90% using passive selection method (Stem-Cell) from primary samples that we used for our experiments ±SD (33 MM and 14 MGUS patients). MM1s cells were used as positive control and the non selected cells as the negative control. M) Western analysis showing p53 and MDM2 expression after Nutlin-3a overnight treatment in 3 different patients, 2 with TP53 deletion (Pt-1 and Pt-2) and 1 with WT (Normal) TP53 (Pt3). CDKN1A mRNA expression by RT-PCR in CD-138+ PCs obtained from 8 different patients (Pt-1-Pt-8 Table S3) after 12 h of Nutlin-3a treatment (N). The PCR product was normalized to ACTIN mRNA expression. The bar-graph represents the mean values observed in four separate studies ± SE. (O) miR-194, miR-192, miR-215 and miR-34a expression in primary tumor samples, after Nutlin-3a treatment, measured by stem loop qRT-PCR. Lines represent relative fold-changes between DMSO and Nutlin-3a treatment. Stem loop q-RT-PCR values were normalized to RNU44 expression. The bar graphs in Figure C and D are representative of the 8 samples used for primary culture and Nutlin-3a treatments. Values were normalized to RN U44 expression. The bar graph in Figure N and O are representative of 8 samples used for primary culture and Nutlin-3a treatments. Values represent mean ± SD from three experiments.

Figure S2. p53 interacts with p53 consensus sequence up-stream of miR-194-1-215 cluster on chromosome 1(q41) in MM cells. Chip assay with anti-p53 or normal IgG from the same animal after 24 hr of p53 non genotoxic activation, revealed binding of p53 to the miR-194-1-215 cluster promoter *in vivo* in MM1s cells. ChIP primers were designed to amplify the region containing the putative p53 binding site in the pri-miR-194-1-215 promoter (-2.7 kb from the cluster). p53-responsive *CDKN1A* gene promoter associated with p53 was used as positive control, whereas amplification of a MT-RNR2 gene portion yielded very little background signals and served as negative control.

Figure S3. miR-192, 194 and 215 regulate *CDKN1A* and *MDM2* mRNA levels in MM cells. (A-C) MM1s, NCI-H929, KMS28BM and RPMI-8226 cells (pre-miRNA-192, 194, 215, Scr sequence– transfected) were harvested at 48 hr after transfection and *CDKN1A* (A), *TP53* (B) and *MDM2* (C) mRNA expression level was assessed. The PCR products for the genes were normalized to ACTIN mRNA expression. The bar-graphs represent mean values observed in four separate studies \pm SD. (D) miRNA-192-194 and 215 effects on *MDM2* protein level in Mut *TP53* cells (RPMI-8226). RPMI-8226 cells (miRNA-192, 194, 215, Scr sequence-transfected) were harvested at 72 h after transfection. Whole cell lysates were subjected to Western blot using *MDM2* and *Gapdh* antibodies. Bars indicate *MDM2* protein relative fold change \pm SD. *Gapdh* was internal loading control and used for the densitometry analysis. The experiment was performed in triplicate.

Figure S4. miR-192, 194 and 215 target human *MDM2* (*HDM2*). (A-B) Assessment of expression of miRNAs in MM transfected cells using pre-miR-192, 194 and 215 and anti-sense oligo-nucleotides (ASOs). MM1s and NCI-H929 cells transfected with pre-miRNAs (A) or ASOs. (B) were harvested at 72 hr after transfection and the level of the microRNAs was assessed by stem loop q-RT-PCR for each miRNA compared to the Scr sequence-transfected cells. Bar-graphs represent the mean values observed in four separate studies \pm SD. (C) Representation of the full length human *MDM2* mRNA (*HDM2*) (D-G) miRNAs predicted to interact with *HDM2* mRNA at several consensus binding sites in its 3'-UTR, according to "in silico" RNA-22 prediction software with a folding energy $>$ -27 Kcal/mol. The MREs are indicated by the triangles. (H-K) Luciferase assay showing decreased luciferase activity in cells co-transfected with pGL3-*MDM2*-3'UTR containing the specific binding sites (~1 kb) for each miRNA. Specifically: CS2117 and CS5974 constructs for miR-194 (H-J) and CS3975 and CS6360 constructs for miR-192 and 215 (I-K). Deletion of six bases in all putative consensus sequences abrogates this effect (Del). Bars indicate firefly luciferase activity normalized to Renilla luciferase activity \pm SD.

Figure S5. miR-192 and 215 target IGF-1 and IGF-1R in MM cells. (A-D) Effect of Nutlin-3a treatment on IGF-R and IGF-1 protein expression in MM cells with different *TP53* status. WT *TP53* (MM1s and NCI-H929) (A-B) and Mutant *TP53* (RPMI-8226 and U266) (C-D) cells were treated with Nutlin-3a (10 μ M) or DMSO vehicle and whole cell lysates collected at different time points were immunoblotted using antisera against IGF-1R, IGF-1, p53, *MDM2*. *Gapdh* was used as loading control. A decrease in IGF-R and IGF-1 protein level is shown only in *TP53* WT cells upon Nutlin-3a treatment. (E) Representation of the full length *IGF-1R* mRNA. (F-G) miRNAs predicted to interact with *IGF-1R* gene in several consensus binding sites at its 3'-UTR, according to "in silico" RNA-22 prediction software with a folding energy $>$ -27 Kcal/mol. (H-I) Luciferase assay showing decreased luciferase activity in cells co-transfected with 2 different constructs (1 kb each) of pGL3-*IGF-1R*-3'UTR and miR-215 (H-I) and miR-192 (I) but not with miR-194 and Scr sequence (H-I). Deletion of six bases in all putative consensus sequences abrogates this effect (Del) (H-I). Bars indicate firefly luciferase activity normalized to Renilla luciferase activity \pm SD.

Figure S6. miR-192 and 215 affect the ability of MM cells to adhere and migrate in response to IGF-1. (A-B) MM1s and RPMI-8226 cells (pre-miRNA-192, 194, 215, Scr sequence–transfected) at 48 hr after transfection were harvested, treated with calcein and incubated with IGF-1 (50 ng/ml) and their ability to adhere to fibronectin plates was assessed by fluorescence assay. MM1s (A) and RPMI-8226 (B) with ectopic re-expression of miR-192, 215 and also miR-194 lost their ability to respond to IGF-1 treatment compare to Scr sequence. (C) Intra-epithelial migration assay in MM1s and RPMI-8226 cells (pre-miRNA-192, 194, 215, Scr–transfected) using HS-27A stromal cell as cellular layer at different concentrations of IGF-1 as attractant. Bars indicate relative fold change of migration compared with the control. All experiments were performed in triplicate \pm SD.

Figure 7. The promoter region of miR-194-2&192 is methylated in MM cell lines. (A) Representation of the genomic region of miR-194-2&192 obtained from University of California Santa Cruz genome browser (2006). The red arrow is the region that we analyzed for the methylation study, including the p53 consensus sequence. (B) Combined bisulfite restriction analysis (COBRA) in 9 MM cell lines. Universal methylated DNA from Millipore was used as positive control and normal CD-138+ plasma cells as negative control. The digestion of PCR products coming from methylated DNA was carried out with TaqI for the region R. (C) stem-loop q-RT-PCR for miR-192 and miR-194 and RT-PCR for *SOCS-1* genes normalized to RN44 and *ACTIN* respectively, expressed as fold increases after 3 days of treatment with 5-Azacytidine (10 μ M) compared to DMSO treated cells. All experiments were performed in triplicate. \pm SD. (D) Illustration of the p53—miR-192,194,215 —MDM2 auto regulatory loops, showing the central role played by the miRs in determining the balance of p53 suppressor and the MDM2 oncoprotein expression levels.

Table S1. miRNAs differentially expressed between WT *TP53* versus Mutant *TP53* MM cell lines. Related to Figure 1

Table S2. miRNAs differentially expressed between MM 1s cells Nutlin-3a treated versus MM1s cells DMSO treated. Related to Figure 1

Table S3. Patient samples clinical data. Related to Figure 1

Bibliography

1. Bartel D. MicroRNAs: Genomics, biogenesis, mechanism, and function. *Cell*. 2004;116:281–297.
2. Braun CJ, Zhang X, Savelyeva I, Wolff S, Moll UM, Schepeler T, Ørntoft TF, Andersen CL, Dobbstein M. p53-Responsive microRNAs 192 and 215 are capable of inducing cell cycle arrest. *Cancer Res*. 2008;68:10094–10104.
3. Chang TC, Yu D, Lee YS, Wentzel EA, Arking DE, West KM, Dang CV, Thomas-Tikhonenko A, Mendell JT. Widespread microRNA repression by Myc contributes to tumorigenesis. *Nat Genet*. 2008;40:43–50.
4. Chng WJ, Glebov O, Bergsagel PL, Kuehl WM. Genetic events in the pathogenesis of multiple myeloma. *Best Pract Res Clin Haematol*. 2007;20:571–596.
5. Croce CM. Oncogenes and cancer. *New England Journal of Medicine*. 2008;358:502–511.
6. Danovi D, Meulmeester E, Pasini D, Migliorini D, Capra M, Frenk R, De Graaf P, Francoz S, Gasparini P, Gobbi A, et al. Amplification of Mdmx (or Mdm4) directly contributes to tumor formation by inhibiting p53 tumor suppressor activity. *Mol Cell Biol*. 2004;24:5835–5843.

7. Dickens MP, Fitzgerald R, Fischer PM. Small-molecule inhibitors of MDM2 as new anticancer therapeutics. *Semin Cancer Biol.* 2009;20:10–18.
8. Fonseca R, Bergsagel PL, Drach J, Shaughnessy J, Gutierrez N, Stewart AK, Morgan G, Van Ness B, Chesi M, Minvielle S, et al. International Myeloma Working Group molecular classification of multiple myeloma: spotlight review. *Leukemia.* 2009;23:2210–2221.
9. Froment P, Dupont J, Christophe-Marine J. Mdm2 exerts pro-apoptotic activities by antagonizing insulin-like growth factor-I-mediated survival. *Cell Cycle.* 2008;7:3098–3103.
10. Galm O, Yoshikawa H, Esteller M, Osieka R, Herman JG. SOCS-1, a negative regulator of cytokine signaling, is frequently silenced by methylation in multiple myeloma. *Blood.* 2002;101:2784–2788.
11. Georges SA, Biery MC, Kim SY, Scheltemer JM, Guo J, Chang AN, Jackson AL, Carleton MO, Linsley PS, Cleary MA, et al. Coordinated regulation of cell cycle transcripts by p53-Inducible microRNAs, miR-192 and miR-215. *Cancer Res.* 2008;68:10105–10112.
12. Girnita L, Girnita A, Larsson O. Mdm2-dependent ubiquitination and degradation of the insulin-like growth factor 1 receptor. *Proc Natl Acad Sci USA.* 2003;100:8247–8252.
13. Gutiérrez NC, Sarasquete ME, Misiewicz-Krzeminska I, Delgado M, De Las Rivas J, Ticona FV, Fermiñán E, Martín-Jiménez P, Chillón C, Risueño A, et al. Deregulation of microRNA expression in the different genetic subtypes of multiple myeloma and correlation with gene expression profiling. *Leukemia.* 2010;24:629–637.
14. Garofalo M, Di Leva G, Romano G, Nuovo G, Suh SS, Ngankea A, Taccioli C, Pichiorri F, Alder H, Secchiero P, et al. miR-221&222 regulate TRAIL resistance and enhance tumorigenicity through PTEN and TIMP3 downregulation. *Cancer Cell.* 2009;16:498–509.
15. He L, He X, Lowe SW, Hannon GJ. microRNAs join the p53 network--another piece in the tumour-suppression puzzle. *Nat Rev Cancer.* 2007;7:819–822.
16. Hermeking H. The miR-34 family in cancer and apoptosis. *Cell Death Differ.* 2010;17:193–199.
17. Hino K, Tsuchiya K, Fukao T, Kiga K, Okamoto R, Kanai T, Watanabe M. Inducible expression of microRNA-194 is regulated by HNF-1alpha during intestinal epithelial cell differentiation. *RNA.* 2008;14:1433–1442.
18. Junttila MR, Evan GI. p53--a Jack of all trades but master of none. *Nat Rev Cancer.* 2009;9:821–829.
19. Krek A, Grün D, Poy MN, Wolf R, Rosenberg L, Epstein EJ, MacMenamin P, da Piedade I, Gunsalus KC, Stoffel M, et al. Combinatorial microRNA target prediction. *Nat Genet.* 2005;37:495–500.
20. Kuehl WM, Bergsagel PL. Multiple myeloma: evolving genetic events and host interactions. *Nature Rev Cancer.* 2002;2:175–187.
21. Lane D. How cells choose to die. *Nature.* 2001;414:25–27.
22. Lewis B, Shih I, Jones-Rhoades M, Bartel D, Burge C. Prediction of mammalian microRNA targets. *Cell.* 2003;115:787–798.

23. Lionetti M, Biasiolo M, Agnelli L, Todoerti K, Mosca L, Fabris S, Sales G, Deliliers GL, Bicciato S, Lombardi L, et al. Identification of microRNA expression patterns and definition of a microRNA/mRNA regulatory network in distinct molecular groups of multiple myeloma. *Blood*. 2009;114:20–26.
24. Marine JC, Lozano G. Mdm2-mediated ubiquitylation: p53 and beyond. *Cell Death Differ*. 2010;17:93–102.
25. Miranda KC, Huynh T, Tay Y, Ang YS, Tam WL, Thomson AM, Lim B, Rigoutsos I. A pattern-based method for the identification of microRNA binding sites and their corresponding heteroduplexes. *Cell*. 2006;126:1203–1217.
26. Park SY, Lee JH, Ha M, Nam JW, Kim VN. miR-29 miRNAs activate p53 by targeting p85 alpha and CDC42. *Nat Struct Mol Biol*. 2009;16:23–29.
27. Ooi MG, Hayden PJ, Kotoula V, McMillin DW, Charalambous E, Daskalaki E, Raje NS, Munshi NC, Chauhan D, Hideshima T, Buon L, Clynes M, et al. Interactions of the Hdm2/p53 and proteasome pathways may enhance the antitumor activity of bortezomib. *Clin Cancer Res*. 2009;5:7153–7160.
28. Pichiorri F, Suh SS, Ladetto M, Kuehl M, Palumbo T, Drandi D, Taccioli C, Zanesi N, Alder H, Hagan JP. MicroRNAs regulate critical genes associated with multiple myeloma pathogenesis. *Proc Natl Acad Sci USA*. 2008;105:12885–12890.
29. Qiang YW, Yao L, Tosato G, Rudikoff S. Insulin-like growth factor I induces migration and invasion of human multiple myeloma cells. *Blood*. 2004;103:301–308.
30. Quesnel B, Preudhomme C, Oscier D, Lepelley P, Collyn-d'Hooghe M, Facon T, Zandecki M, Fenaux P. Over-expression of the MDM2 gene is found in some cases of haematological malignancies. *Br J Haematol*. 1994;88:415–418.
31. Roccaro AM, Sacco A, Thompson B, Leleu X, Azab AK, Azab F, Runnels J, Jia X, Ngo HT, Melhem MR, et al. MicroRNAs 15a and 16 regulate tumor proliferation in multiple myeloma. *Blood*. 2009;113:6669–6680. Thompson B et al.
32. Saha MN, Chang H. Pharmacological activation of the p53 pathway in haematological malignancies. *J Clin Pathol*. 2010;63:204–209.
33. Shangary S, Qin D, McEachern D, Liu M, Miller RS. Temporal activation of p53 by a specific MDM2 inhibitor is selectively toxic to tumors and leads to complete tumor growth inhibition. *Proc Natl Acad Sci U S A*. 2008;105:3933–3938.
34. Sinha AU, Kaimal V, Chen J, Jegga AG. Dissecting microregulation of a master regulatory network. *BMC Genomics*. 2008;23:88.
35. Song B, Wang Y, Kudo K, Gavin EJ, Xi Y, Ju J. miR-192 Regulates dihydrofolate reductase and cellular proliferation through the p53-microRNA circuit. *Clin Cancer Res*. 2008;14:8080–8086.
36. Stühmer T, Bargou RC. Selective pharmacologic activation of the p53-dependent pathway as a therapeutic strategy for hematologic malignancies. *Cell Cycle*. 2006;5:39–42.

37. Tai YT, Podar K, Catley L, Tseng YH, Akiyama M, Shringarpure R, Burger R, Hideshima T, Chauhan D, Mitsiades N, et al. Insulin-like growth factor-1 induces adhesion and migration in human multiple myeloma cells via activation of beta1-integrin and phosphatidylinositol 3'-kinase/AKT signaling. *Cancer Res.* 2003;63:5850–5858.
38. Teoh G, Urashima M, Ogata A, Chauhan D, DeCaprio JA, Treon SP, Schlossman RL, Anderson KC. MDM2 protein overexpression promotes proliferation and survival of multiple myeloma cells. *Blood.* 1997;90:1982–1992.
39. Weiss BM, Abadie J, Verma P, Howard RS, Kuehl WM. A monoclonal gammopathy precedes multiple myeloma in most patients. *Blood.* 2009;113:5418–5422.
40. Ventura A, Kirsch DG, McLaughlin ME, Tuveson DA, Grimm J, Lintault L, Newman J, Reczek EE, Weissleder R, Jacks T. Restoration of p53 function leads to tumour regression in vivo. *Nature.* 2007;445:661–665.
41. Ventura A, Young AG, Winslow MM, Lintault L, Meissner A, Erkeland SJ, Newman J, Bronson RT, Crowley D, Stone JR, et al. Targeted deletion reveals essential and overlapping functions of the miR-17 through 92 family of miRNA clusters. *Cell.* 2008;132:875–886.
42. Xue W, Zender L, Miething C, Dickins RA, Hernando E, Krizhanovskiy V, Cordon-Cardo C, Lowe SW. Senescence and tumour clearance is triggered by p53 restoration in murine liver carcinomas. *Nature.* 2007;445:656–660.
43. Zhang Y, Gao JS, Tang X, Tucker LD, Quesenberry P, Rigoutsos I, Ramratnam B. MicroRNA 125a and its regulation of the p53 tumor suppressor gene. *FEBS Lett.* 2009;583:3725–3730.